

Weight Assignment using Entropy

Qian Yurong¹ and Gwanggil Jeon²

¹Software College, Xinjiang University Urumqi 830008, P. R. China

²Department of Embedded Systems Engineering, Incheon National University
119 Academy-ro, Yeonsu-gu, Incheon 406-772, Korea
qyr@xju.edu.cn, gjeon@inu.ac.kr

Abstract

In this paper, a compromised method is presented for the interlaced signals. The interlaced signals are vertically reconstructed by interpolation method. The efficient edge directed line average method is the advanced version of edge directed line average method, which uses two more useful metrics to assess edge direction. On the other hand, Bob method does not consider edge direction, rather its results are the average results of upper and lower lines. We used information entropy to give weights. Considered two methods were efficient edge directed line average and Bob methods, and we obtain compromised approach. Experimental results show that the presented method provides satisfactory results.

Keywords: Color image, information entropy, down-sampling, edge map

1. Introduction

Video processing uses spatial and temporal information to restore missing information [1-5]. Sometimes, each information is used separately, or sometimes is used mixed fashion [6-7]. The interlaced signal has been used for many years [8]. Although many issues have been studied, however there are still some open issues to be solved [9-10].

One of the simplest methods is Bob method, which restore a missing line between two neighbor pixels existing in the interlaced images before displaying an image [11]. Although methods based on temporal information give better performance, but normally their complexity is higher than spatial methods because motion models and trajectories are needed. However, spatial domain methods only use give single field, therefore these methods are widely used in many cases for their simplicity.

One of widely used methods is the famous edge-based line average method which uses correlations in three directions between pixels in upper and lower lines [12]. More recently, efficient edge directed line average method was proposed [13-15].

The rest of this paper is outlined as follows. The efficient edge directed line average method is explained in Section 2. In this section, proposed method and entropy map are introduced as well. Section 3 shows objective and subjective performance comparison. Simulation results for a McM dataset are presented in Section 4. Finally, concluding remarks are presented in Section 5.

2. Proposed Method

The figure of edge directed line average method is shown in Figure 1.

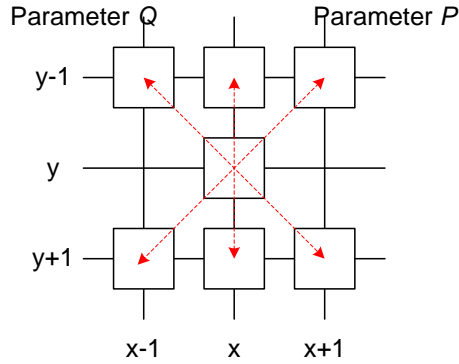


Figure 1. Flowchart of Edge Directed Line Average Method. P and Q are Dominant Edge Direction Selector

The edge detector of edge directed line average method is computed as Eqs. (1) and (2).

$$P = |k(x-1, y-1) - k(x+1, y+1)|, \quad (1)$$

$$Q = |k(x-1, y+1) - k(x+1, y-1)|, \quad (2)$$

In efficient edge directed line average method, two parameters P and Q are calculated as Eqs. (3) and (4).

$$P = |k(x-1, y) - k(x+1, y+1)| + |k(x-1, y-1) - k(x+1, y)|, \quad (3)$$

$$Q = |k(x-1, y+1) - k(x+1, y)| + |k(x-1, y) - k(x+1, y-1)|, \quad (4)$$

This equation can be drawn in Figure 2.

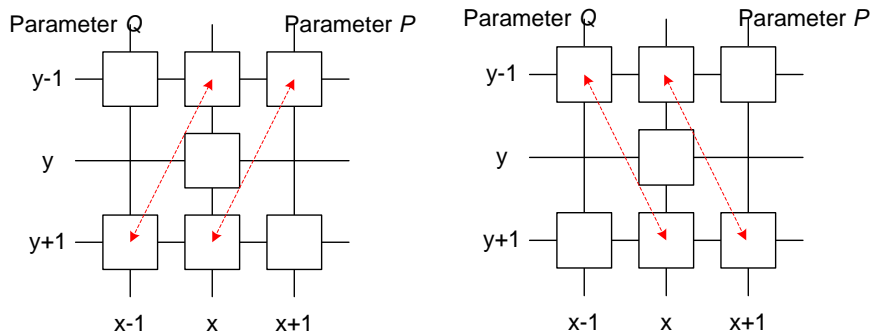


Figure 2. Flowchart of Efficient Edge Directed Line Average Method P and Q are Dominant Edge Direction Selector

The entropy is an assessment of order and disorder in information theory. This concept was originally proposed by Claude E. Shannon, and we consider his entropy as a weight assignment metric for the information. The Shannon's entropy of event A is obtained as,

$$H(A) = - \sum_{i=1}^n P(a_i) \log_b P(a_i). \quad (5)$$

Where b is the basis of log. When $b=2$, results are shown in bit, and when $b=10$, results are shown in decimal value. Using this equation, we obtain edge map as shown in Figure 3.



Figure 3. (a) Original #16 McM Image (b) Entropy Map

The block diagram of the proposed method is introduced in Figure 4.

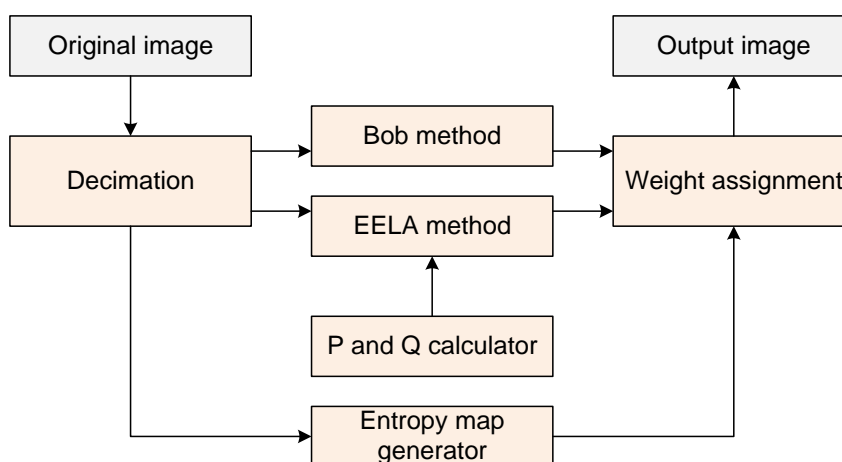


Figure 4. Block Diagram of the Proposed Method

The procedure of the proposed method is as follows:

Step 1 Obtain RGB images. This image is decomposed into three channels, Y, Cb, and Cr. Y is luminance information and Cb, Cr are chrominance information.

Step 2 Decimation process is applied to Y channel.

Step 3 There are two methods to restore interlaced images: one is Bob method and the other is EELA method.

Step 4 To perform EELA method, one has to calculate P and Q parameters using Eqs. (3) and (4).

Step 5 Obtain the edge map from decimated Y channel. This map is used as weight function.

Step 6 Using the result of Step 5, weighted average value of Bob and EELA are computed.

Step 7 Finally, output image is obtained.

As described in Introduction section, we use two conventional methods for our proposed system. First of all, we vertically decimate the original signal image. This image we consider interlaced image. Now, entropy map is obtained using Shannon's entropy

equation Eq. (5). The output value of entropy should be ranging 0 and 1, therefore normalization is applied. We bring threshold parameter ζ , which is used as,

$$\begin{aligned} &\text{If entropy is bigger than } \zeta, \text{ then Bob method is used.} \\ &\text{Otherwise, EELA method is used.} \end{aligned} \quad (5)$$

Empirically, we found suitable ζ values range from 0.1 to 0.7.

3. Experimental Results

Extensive experiments have been conducted to assess performance of the proposed method. Objective and subjective performance comparison is provided in this section. We used 500-by-500 size 18 McM images for the comparison. To conduct experiments, all images were separated into even and odd fields and we used deinterlacing approaches. Two conventional methods were used, bob methods (M_1) and EELA methods (M_2).

To assess objective performance, four test images were used: #12, #13, #14, and #16. Figure 5 shows results images of #12 image, where one can find original image in (a), entropy image in (b), M_1 result in (c), M_2 result in (d), proposed method result in (e), difference between original and M_1 result in (f), and difference between original and M_2 result in (g). From provided comparison, we understand the proposed method gives better visual effect although it is compromised result of M_1 and M_2 . In addition, details were well survived and edge region were well preserved.

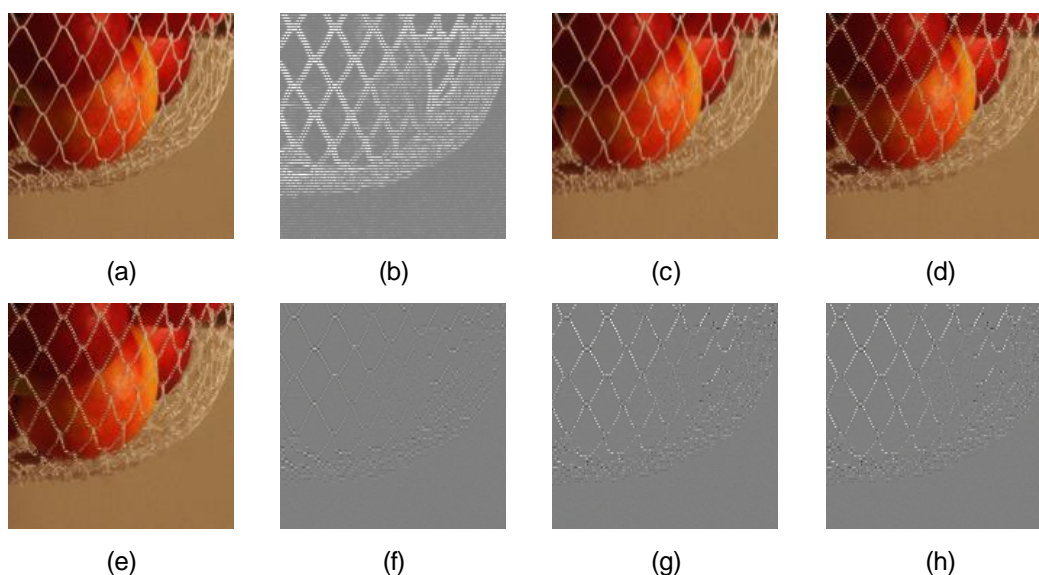


Figure 5. McM Image #12: (a) Original Image, (b) Entropy Map, (c) M_1 Result, (d) M_2 Result, (e) Proposed Method, (f) Difference between Original and M_1 , (g) Difference between Original and M_2 , and (h) Difference between Original and Proposed Method

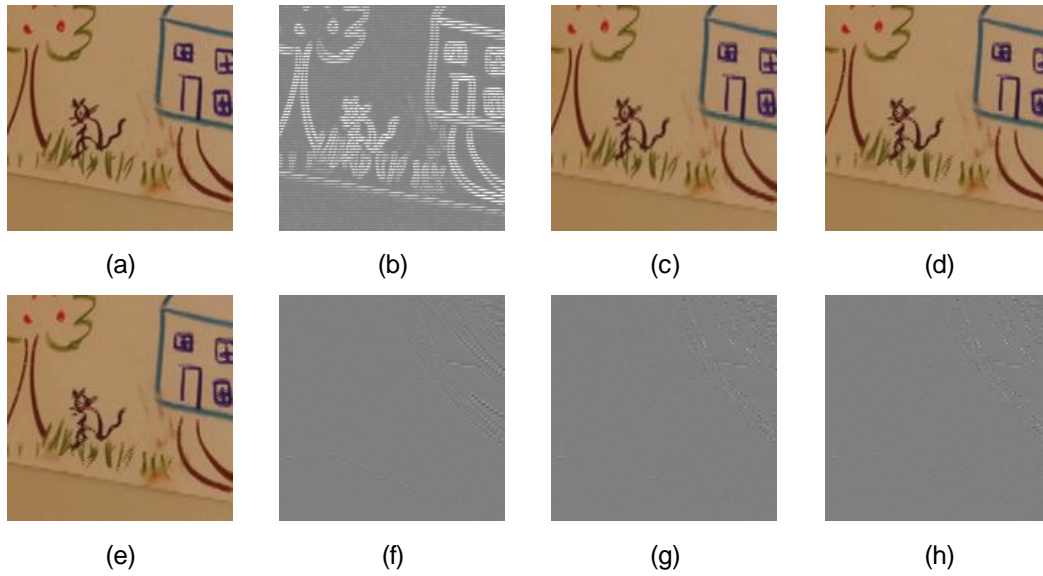


Figure 6. McM Image #13: (a) Original Image, (b) Entropy Map, (c) M_1 Result, (d) M_2 Result, (e) Proposed Method, (f) Difference between Original and M_1 , (g) Difference between Original and M_2 , and (h) Difference between Original and Proposed Method

In the same manner, one can find similar results in Figs. 6-8. McM image #13 was tested. Similarly, the image was first vertically downsampled by a factor of 2, and then it was restored by M_1 , M_2 , and the proposed method

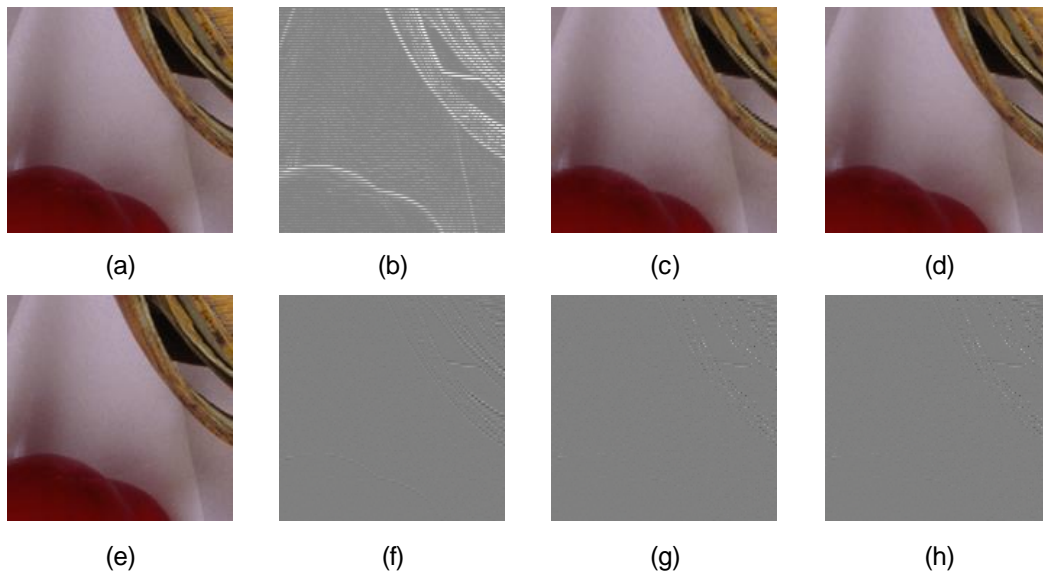


Figure 7. McM Image #14: (a) Original Image, (b) Entropy Map, (c) M_1 Result, (d) M_2 Result, (e) Proposed Method, (f) Difference between Original and M_1 , (g) Difference between Original and M_2 , and (h) Difference between Original and Proposed Method

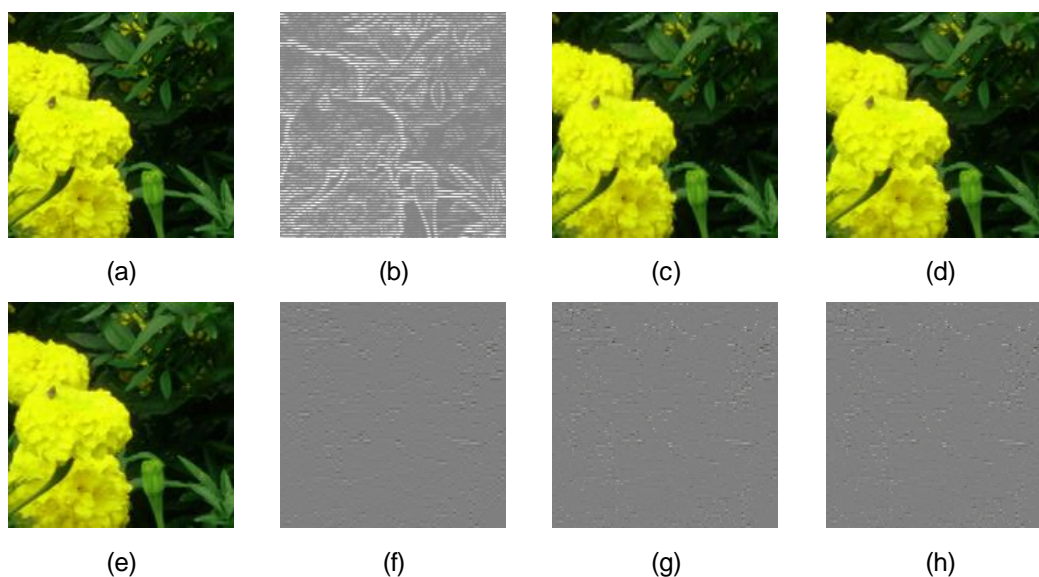


Figure 8. McM Image #16: (a) Original Image, (b) Entropy Map, (c) M₁ Result, (d) M₂ Result, (e) Proposed Method, (f) Difference between Original and M₁, (g) Difference between Original and M₂, and (h) Difference between Original and Proposed Method

To assess numerical result of image quality, we computed CPSNR: PSNR in red channel, PSNR in green channel, and PSNR in blue channel, which are shown in Tables 1-4. As to objective performance, the presented method provides the appropriate PSNR results.

Table 1. CPSNR Results for 18 McM Images

| ξ | 0.1 | 0.2 | 0.3 | 0.4 | 0.5 | 0.6 |
|-------|-------|-------|-------|-------|-------|-------|
| 1 | 28.69 | 28.36 | 27.87 | 27.60 | 27.36 | 27.33 |
| 2 | 33.86 | 32.85 | 31.93 | 31.48 | 31.18 | 31.21 |
| 3 | 27.78 | 27.40 | 26.84 | 26.29 | 25.92 | 25.87 |
| 4 | 29.51 | 29.21 | 28.95 | 28.84 | 28.89 | 29.03 |
| 5 | 32.07 | 31.47 | 31.00 | 30.51 | 30.52 | 30.53 |
| 6 | 38.61 | 38.39 | 37.96 | 37.66 | 37.60 | 37.65 |
| 7 | 34.33 | 33.64 | 33.02 | 32.48 | 32.37 | 32.37 |
| 8 | 31.84 | 31.72 | 31.61 | 31.44 | 31.17 | 31.18 |
| 9 | 36.21 | 36.00 | 36.16 | 36.49 | 37.09 | 37.15 |
| 10 | 37.34 | 36.13 | 35.70 | 35.52 | 35.49 | 35.48 |
| 11 | 38.91 | 38.50 | 38.37 | 38.42 | 38.53 | 38.53 |
| 12 | 33.35 | 31.24 | 29.46 | 28.43 | 27.84 | 27.81 |
| 13 | 35.53 | 34.76 | 34.21 | 33.92 | 33.67 | 33.67 |
| 14 | 39.74 | 39.16 | 39.21 | 39.67 | 39.90 | 39.91 |
| 15 | 49.53 | 49.37 | 49.36 | 49.37 | 49.37 | 49.37 |
| 16 | 33.58 | 33.34 | 33.14 | 32.95 | 33.01 | 33.07 |
| 17 | 35.65 | 35.18 | 34.74 | 34.39 | 34.33 | 34.30 |
| 18 | 39.91 | 39.52 | 38.23 | 37.26 | 36.82 | 36.73 |
| Avg. | 35.36 | 34.79 | 34.32 | 34.04 | 33.95 | 33.96 |

Table 2. Red Channel PSNR Results for 18 Mcm Images

| ξ | 0.1 | 0.2 | 0.3 | 0.4 | 0.5 | 0.6 |
|-------|-------|-------|-------|-------|-------|-------|
| 1 | 28.70 | 28.42 | 28.02 | 27.79 | 27.49 | 27.44 |
| 2 | 33.86 | 32.85 | 31.93 | 31.47 | 31.18 | 31.20 |
| 3 | 27.77 | 27.40 | 26.83 | 26.27 | 25.90 | 25.85 |
| 4 | 29.51 | 29.21 | 28.95 | 28.84 | 28.89 | 29.03 |
| 5 | 32.10 | 31.51 | 31.07 | 30.60 | 30.61 | 30.62 |
| 6 | 38.61 | 38.39 | 37.96 | 37.66 | 37.60 | 37.65 |
| 7 | 34.31 | 33.62 | 33.01 | 32.47 | 32.35 | 32.36 |
| 8 | 31.83 | 31.72 | 31.60 | 31.41 | 31.12 | 31.12 |
| 9 | 36.19 | 35.98 | 36.13 | 36.45 | 37.02 | 37.09 |
| 10 | 37.29 | 36.09 | 35.66 | 35.48 | 35.45 | 35.45 |
| 11 | 38.74 | 38.31 | 38.19 | 38.25 | 38.36 | 38.36 |
| 12 | 33.35 | 31.24 | 29.45 | 28.43 | 27.84 | 27.80 |
| 13 | 35.53 | 34.76 | 34.21 | 33.92 | 33.67 | 33.67 |
| 14 | 39.74 | 39.16 | 39.21 | 39.67 | 39.90 | 39.91 |
| 15 | 49.51 | 49.29 | 49.29 | 49.30 | 49.30 | 49.30 |
| 16 | 33.22 | 32.98 | 32.74 | 32.49 | 32.53 | 32.60 |
| 17 | 35.62 | 35.15 | 34.69 | 34.31 | 34.25 | 34.23 |
| 18 | 39.90 | 39.51 | 38.17 | 37.19 | 36.74 | 36.65 |
| Avg. | 35.32 | 34.76 | 34.28 | 34.00 | 33.90 | 33.91 |

Table 3. Green Channel PSNR Results for 18 Mcm Images

| ξ | 0.1 | 0.2 | 0.3 | 0.4 | 0.5 | 0.6 |
|-------|-------|-------|-------|-------|-------|-------|
| 1 | 28.48 | 28.11 | 27.55 | 27.24 | 26.94 | 26.89 |
| 2 | 33.83 | 32.82 | 31.90 | 31.45 | 31.15 | 31.18 |
| 3 | 27.77 | 27.40 | 26.83 | 26.27 | 25.90 | 25.85 |
| 4 | 29.51 | 29.21 | 28.95 | 28.84 | 28.89 | 29.03 |
| 5 | 32.05 | 31.46 | 30.97 | 30.47 | 30.47 | 30.48 |
| 6 | 38.61 | 38.39 | 37.96 | 37.66 | 37.60 | 37.65 |
| 7 | 34.33 | 33.65 | 33.03 | 32.49 | 32.37 | 32.37 |
| 8 | 31.83 | 31.72 | 31.60 | 31.41 | 31.12 | 31.12 |
| 9 | 36.19 | 35.98 | 36.13 | 36.45 | 37.02 | 37.09 |
| 10 | 37.29 | 36.09 | 35.66 | 35.48 | 35.45 | 35.44 |
| 11 | 38.74 | 38.31 | 38.19 | 38.25 | 38.36 | 38.36 |
| 12 | 33.35 | 31.24 | 29.45 | 28.43 | 27.84 | 27.80 |
| 13 | 35.53 | 34.76 | 34.21 | 33.92 | 33.67 | 33.67 |
| 14 | 39.74 | 39.16 | 39.21 | 39.67 | 39.90 | 39.91 |
| 15 | 49.51 | 49.35 | 49.35 | 49.36 | 49.36 | 49.36 |
| 16 | 33.22 | 32.98 | 32.74 | 32.48 | 32.52 | 32.59 |
| 17 | 35.63 | 35.16 | 34.71 | 34.33 | 34.27 | 34.24 |
| 18 | 39.90 | 39.51 | 38.18 | 37.20 | 36.74 | 36.65 |
| Avg. | 35.31 | 34.74 | 34.26 | 33.97 | 33.87 | 33.87 |

Table 4. Blue Channel PSNR Results for 18 Mcm Images

| ξ | 0.1 | 0.2 | 0.3 | 0.4 | 0.5 | 0.6 |
|-------|-------|-------|-------|-------|-------|-------|
| 1 | 28.91 | 28.56 | 28.06 | 27.79 | 27.69 | 27.68 |
| 2 | 33.89 | 32.88 | 31.97 | 31.51 | 31.21 | 31.24 |
| 3 | 27.79 | 27.42 | 26.88 | 26.33 | 25.96 | 25.91 |
| 4 | 29.51 | 29.21 | 28.95 | 28.84 | 28.89 | 29.03 |

| | | | | | | |
|------|-------|-------|-------|-------|-------|-------|
| 5 | 32.05 | 31.46 | 30.97 | 30.47 | 30.48 | 30.48 |
| 6 | 38.61 | 38.39 | 37.96 | 37.66 | 37.60 | 37.65 |
| 7 | 34.34 | 33.65 | 33.04 | 32.49 | 32.38 | 32.38 |
| 8 | 31.85 | 31.74 | 31.63 | 31.50 | 31.27 | 31.30 |
| 9 | 36.25 | 36.06 | 36.23 | 36.58 | 37.22 | 37.29 |
| 10 | 37.44 | 36.23 | 35.79 | 35.60 | 35.57 | 35.57 |
| 11 | 39.28 | 38.90 | 38.75 | 38.78 | 38.89 | 38.89 |
| 12 | 33.35 | 31.25 | 29.46 | 28.44 | 27.84 | 27.81 |
| 13 | 35.53 | 34.76 | 34.21 | 33.92 | 33.67 | 33.67 |
| 14 | 39.74 | 39.16 | 39.21 | 39.67 | 39.90 | 39.91 |
| 15 | 49.56 | 49.46 | 49.46 | 49.47 | 49.47 | 49.47 |
| 16 | 34.39 | 34.17 | 34.08 | 34.04 | 34.18 | 34.22 |
| 17 | 35.70 | 35.23 | 34.83 | 34.52 | 34.46 | 34.43 |
| 18 | 39.91 | 39.55 | 38.35 | 37.41 | 36.98 | 36.89 |
| Avg. | 35.45 | 34.89 | 34.43 | 34.17 | 34.09 | 34.10 |



(a)



(b)



(c)



(d)

Figure 9. Visual Performance Comparison on McM Image #1: (a) Original Image, (b) M_1 Result, (c) M_2 Result, and (d) Proposed Method

Tables 1-4 show that the objective performance of M_2 is worse than that of M_1 . However, we found that the visual performance of M_1 is not superior to that of M_2 . Figure 9 shows four images, original zoomed image of McM #1, and its corresponding M_1 , M_2 ,

and proposed method. It can be found that the staircase artifacts of Figure 9(b) is more severe than that of Figure X(c). In addition, image of Figure 9(b) is more blur than M_2 . Therefore, it can be concluded that M_2 gives better visual performance although its metric indicates other results. Figure 9(d) shows the result of proposed method. It can be found that the proposed method gives the best visual performance out of all candidates.

4. Conclusions

This paper studies interlaced to progressive frame rate conversion method. The interlaced signals are vertically reconstructed by interpolation method. Two methods, namely the efficient edge directed line average method and Bob were used in this system. We used information entropy to assign weights. Simulation results show that the presented method provides satisfactory results.

Acknowledgments

This work was supported by the Incheon National University Research Grant in 2013. This paper is a revised and expanded version of a paper entitled "Entropy Map Generation for Image Enhancement" presented at MulGraB2015, November 25-28, 2015 at International Center, Jeju National University, Jeju Island, Korea.

References

- [1] E. B. Bellars and G. D. Haan, "De-interlacing: A Key Technology for Scan Rate Conversion", Elsevier, Amsterdam, (2000).
- [2] G. D. Haan and E. B. Bellars, "Deinterlacing—an overview", Proceedings of the IEEE, vol. 86, no. 9, September (1998), pp. 1839-1857.
- [3] T. Jeong, Y. Kim, K. Sohn and C. Lee, "Deinterlacing with selective motion compensation", Opt. Eng., vol. 45, no. 7, July (2006), pp. 077001.
- [4] T. Chen, H. R. Wu and Z. H. Yu, "Efficient deinterlacing algorithm using edge-based line average interpolation", Opt. Eng., vol. 39, no. 8, August (2000), pp. 2101-2105.
- [5] W. Kim, S. Jin and J. Jeong, "Novel intra deinterlacing algorithm using content adaptive interpolation", IEEE Trans. Cons. Elect., vol. 53, no. 3, August (2007), pp. 1036-1043.
- [6] D. H. Lee, "A new edge-based intra-field interpolation method for deinterlacing using locally adaptive-thresholded binary image", IEEE Trans. Cons. Elect., vol. 54, no. 1, (2008), pp. 110-115.
- [7] P. Y. Chen and Y. H. Lai, "A low-complexity interpolation method for deinterlacing", IEICE Trans. Inf. & Syst., vol. E90-D, no. 2, February (2007).
- [8] C. Shannon, "A mathematical theory of communication", Bell system technical journal, vol. 27, (1948).
- [9] G. Chaitin, "On the Length of Programs for Computing Finite Binary Sequences", J. ACM, vol. 13, no. 4, (1966), pp. 547-569.
- [10] P. Gacs, "On the symmetry of algorithmic information", Soviet Mathematics Doklady, (1974).
- [11] L. Levin, "Laws of Information Conservation (Non-growth) and Aspects of the Foundation of Probability Theory", Prob. Peredachi Inf., vol. 10, no. 3, (1974).
- [12] A. Renyi, "On Measures of Entropy and Information. In Berkeley Symposium Mathematics", Statistics, and Probability, (1960).
- [13] T. Chen, H. R. Wu and Z. H. Yu, "Efficient deinterlacing algorithm using edge-based line average interpolation", Optical Engineering, vol. 39, no. 8, August (2000), pp. 2101-2105.
- [14] G. Jeon, "Contrast Intensification in NTSC YIQ", IJCA, vol. 6, no. 4, August (2013), pp. 157-166.
- [15] G. Jeon, "Measuring and Comparison of Edge Detectors in Color Spaces", IJCA, vol. 6, no. 5, October (2013), pp. 21-30.

Author

Gwanggil Jeon received the BS, MS, and PhD (summa cum laude) degrees in Department of Electronics and Computer Engineering from Hanyang University, Seoul, Korea, in 2003, 2005, and 2008, respectively.

From 2008 to 2009, he was with the Department of Electronics and Computer Engineering, Hanyang University, from 2009 to 2011, he was with the School of

Information Technology and Engineering (SITE), University of Ottawa, as a postdoctoral fellow, and from 2011 to 2012, he was with the Graduate School of Science & Technology, Niigata University, as an assistant professor. He is currently an assistant professor with the Department of Embedded Systems Engineering, Incheon National University, Incheon, Korea. His research interests fall under the umbrella of image processing, particularly image compression, motion estimation, demosaicking, and image enhancement as well as computational intelligence such as fuzzy and rough sets theories. He was the recipient of the IEEE Chester Sall Award in 2007 and the 2008 ETRI Journal Paper Award.